JACS
JOURNAL OF THE AMERICAN CHEMICAL SOCIETY

Communication

pubs.acs.org/JACS

Chiral Phase Transfer and Enantioenrichment of Thiolate-Protected Au_{102} Clusters

Stefan Knoppe,*[,†] O. Andrea Wong,[‡] Sami Malola,[§] Hannu Häkkinen,[§,∥] Thomas Bürgi,[⊥] Thierry Verbiest,[†] and Christopher J. Ackerson*[,‡]

[†]Department of Chemistry, Molecular Imaging and Photonics, KU Leuven, Celestijnenlaan 200D, 3001 Heverlee, Belgium
[‡]Department of Chemistry, Colorado State University, Fort Collins, Colorado 80523, United States
[§]Department of Physics and [∥]Department of Chemistry, Nanoscience Center, University of Jyväskylä, FI-40014 Jyväskylä, Finland
[⊥]Department of Physical Chemistry, University of Geneva, 1211 Geneva 4, Switzerland

Supporting Information

ABSTRACT: The Au_{102}(*p*-MBA)$_{44}$ cluster (*p*-MBA: *para*-mercaptobenzoic acid) is observed as a chiral compound comprised of achiral components in its single-crystal structure. So far the enantiomers observed in the crystal structure are not isolated, nor is the circular dichroism spectrum known. A chiral phase transfer method is presented which allows partial resolution of the enantiomers by the use of a chiral ammonium bromide, (−)-1*R*,2*S*-*N*-dodecyl-*N*-methylephedrinium bromide ((−)-DMEBr). At sufficiently low concentration of (−)-DMEBr, the phase transfer from water to chloroform is incomplete. Both the aqueous and organic phases show optical activity of near mirror image relationship. Differences in the spectra are ascribed to the formation of diastereomeric salts. At high concentrations of (−)-DMEBr, full phase transfer is observed. The organic phase, however, still displays optical activity. We assume that one of the diastereomers has very strong optical activity, which overrules the cancelation of the spectra with opposite sign. Comparison with computations further corroborates the experimental data and allows a provisional assignment of handedness of each fraction.

The structure of the Au_{102}(*p*-MBA)$_{44}$ (*p*-MBA: *para*-mercaptobenzoic acid) cluster[1] is a landmark in several respects. It is not only the first thiolate-protected gold cluster structure solved by direct methods but also provided direct evidence for a thiolate-gold bonding motif that separates gold atoms into two distinct chemical environments, as predicted theoretically.[2] Briefly, the cluster consists of a D_{5h} Au_{79} core which is protected by 19 SR-Au-SR and 2 SR-(Au-SR)$_2$ motifs (Scheme 1). The cluster is intrinsically chiral due to the arrangement of the protecting ligands on the surface of the D_{5h} core of the cluster. Since the *p*-MBA ligand is achiral itself, the cluster crystallizes as a racemate in its unit cell. This type of chirality has also been observed in $Au_{38}(SR)_{24}$[3] and $Au_{28}(SR)_{20}$[4] clusters and is predicted to occur in $Au_{40}(SR)_{24}$.[5,6] While it was possible for the latter species to separate their enantiomers by chiral HPLC and measure their circular dichroism (CD) spectra,[4,5,7] this has, to our knowledge, not been achieved for the Au_{102}(*p*-MBA)$_{44}$ cluster. CD spectra typically resolve more transitions than the ordinary absorption spectra. As for Au:thiolate clusters, the absorption spectra become increasingly featureless with increasing size (for a comparison of different cluster sizes, see Figure 8 in ref 8). The spectrum of the Au_{102}(*p*-MBA)$_{44}$ cluster only shows some weak, poorly resolved features,[9] in strong contrast to the feature-rich spectra of the $Au_{25}(SR)_{18}$ and $Au_{38}(SR)_{24}$ clusters.[10,11] In addition, chirality is an unappreciated aspect of nanocluster structure in the increasingly widespread use of water-soluble thiolate-protected gold clusters in biological applications such as cancer targeting[12] or contrast enhancement.[13,14] The interaction of chiral nanoparticles with chiral biomolecules is essentially uninvestigated, in part because of difficulty in resolving enantiomers of clusters.

We herein present a phase transfer method using a chiral ammonium salt, (−)-1*R*,2*S*-*N*-dodecyl-*N*-methylephedrinium bromide ((−)-DMEBr, Figure 1), to preferably transfer one of the enantiomers of the Au_{102}(*p*-MBA)$_{44}$ cluster from water into a chloroform organic phase. The approach is similar to phase transfer mediated by the widely used tetraoctylammonium bromide. Yao reported on such (chiral) DME-based

Scheme 1. Structures of the Au_{102}(*p*-MBA)$_{44}$ Cluster (left) and the *p*-MBA Ligand (right)[a]

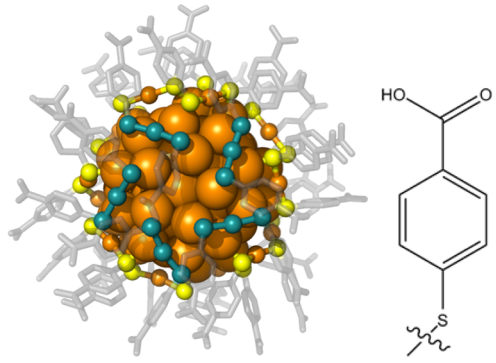

[a]Left-handed enantiomer is shown. Chirality of the protecting units is highlighted in cyan. Coordinates are from ref 15. Au, orange; sulfur, yellow; other, gray.

Received: January 24, 2014
Published: March 4, 2014

   dx.doi.org/10.1021/ja500809p | *J. Am. Chem. Soc.* 2014, 136, 4129−4132

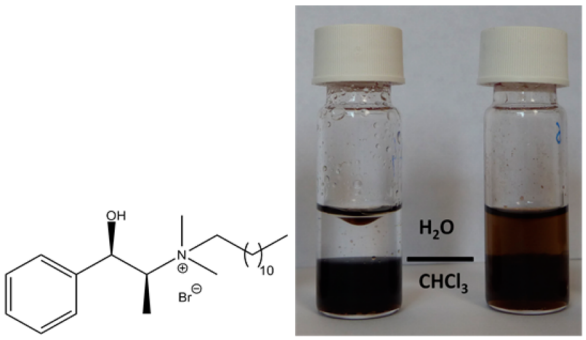

Figure 1. (Left) (−)-DMEBr, the chiral phase transfer agent used to resolve *rac*-Au_{102}(*p*-MBA)$_{44}$ clusters. (Right) Au_{102}(*p*-MBA)$_{44}$ clusters after phase transfer with DMEBr. The left vial shows the clusters after phase transfer at high concentrations of (−)-DMEBr (5.0 mg/mL), the right vial shows the clusters after partial phase transfer with low concentrations of (−)-DMEBr (0.5 mg/mL, see text). The top phase is the aqueous phase, the bottom phase is chloroform.

phase transfer of enantiopure and *rac*-penicillamine-protected gold clusters.[16]

At suitable concentration of (−)-DMEBr (for details, see the Supporting Information), incomplete phase transfer is observed. The two phases were separated, and CD spectra were recorded. Both the aqueous and organic phases exhibit (weak) optical activity in the visible range of the spectrum (Figure 2). A control measurement of the (colorless) (−)-DMEBr in chloroform shows optical activity in the UV only (below 300 nm, Figure S2). We therefore conclude that the optical activity stems from the Au_{102}(*p*-MBA)$_{44}$ clusters. Additional evidence arises in the CD spectra of each phase. The two phases possess an approximately mirror image relationship in the CD spectra, typical of enantiomers. We discuss the deviations from perfect mirror image relationships below.

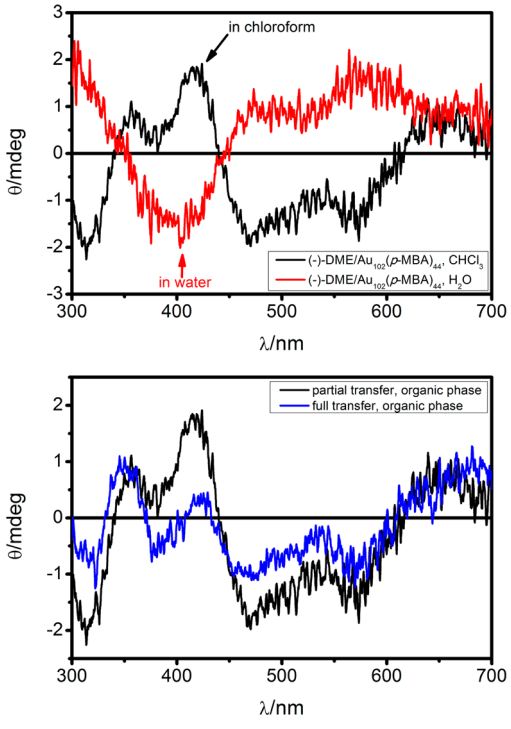

Figure 2. (Top) CD spectra of the organic (black) and aqueous phase (red) after incomplete phase transfer of *rac*-Au_{102}(*p*-MBA)$_{44}$ with (−)-DMEBr (0.5 mg/mL). Both phases display optical activity of nearly mirror image relationship (see text), indicating (partial) resolution of the enantiomers of the cluster. Bottom: CD spectra of partly phase transferred Au_{102}(*p*-MBA)$_{44}$ (black, in chloroform) and fully phase transferred clusters (5.0 mg/mL, blue). The CD spectra of the latter resemble those of the enantioenriched sample.

The CD signals of the two phases indicate a selective transfer of one enantiomer of the cluster. A likely explanation of the observed optical activity after incomplete phase transfer is the formation of ion pairs Au_{102}(*p*-MBA)$_{44}$/(−)-DME$^+$ with different stability depending on the handedness of the Au_{102} cluster. Since the ammonium ion is chiral, the formation of diastereomeric salts (−)-DME/*A*-Au_{102} and (−)-DME/*C*-Au_{102} is expected (where *A*/*C* (anticlockwise/clockwise) to denote the sense of handedness of the protecting units along the principal axis of the cluster). Diastereomers differ in their physical properties, and the formation of diastereomeric ion pairs is commonly used in the resolution of racemic mixtures, e.g., via selective formation and crystallization.[17] Two key features are expected to play a role in the present case: (1) the fact that the protecting ligand bears a carboxylic acid function (which can be deprotonated) and (2) the intrinsic chirality of the cluster due to the arrangement of the protecting $Au_m(SR)_{m+1}$ units on the surface of the cluster core. While the prior provides a suitable source of interaction with the ammonium cation, the latter determines the diastereomeric properties. Due to the different properties of the formed salts, one of the enantiomers of Au_{102}(*p*-MBA)$_{44}$ is expected to selectively interact with the (−)-DME$^+$ ions, hence leading to incomplete phase transfer and partial resolution of the enantiomers. The differences between the diastereomers may account for the deviation from mirror image relationship (e.g., in the 350−400 nm region) in the CD spectra (Figure 2, top). In summary, the observed optical activity of partly phase-transferred clusters is due to a selective transfer of one of the enantiomers. This resolution creates enantiomeric excesses in both phases. Based on the weak CD responses, we assume that the enantiomeric excesses are low as compared to the HPLC separation of $Au_{38}(SCH_2CH_2Ph)_{24}$ and $Au_{40}(SCH_2CH_2Ph)_{24}$ clusters.[7,18]

Yao et al. presented a similar phase transfer using (−)-DMEBr and *R*/*S*-penicillamine-protected gold clusters.[16] Clusters protected with a racemic mixture of the penicillamine (pen) ligand were (fully) transferred from aqueous to the organic phase. For at least one cluster size, optical activity is found in the organic phase, despite the fact that the clusters are protected with a racemic mixture of the ligands. Hence, it was concluded that the chiral counterion plays a pivotal role due to the formation of diastereomeric ion pairs and can induce optical activity via the second coordination sphere (see below). The measured CD spectra of the transferred *rac*-pen-protected clusters resemble those of *S*-pen-protected ones but are weaker. Similarly, a full phase transfer of *rac*-Au_{102}(*p*-MBA)$_{44}$ with (−)-DMEBr leads to optical activity in the organic phase (Figure 2, bottom). One would expect the CD spectra of the diastereomeric ion pairs to cancel to (near) zero; however, we assume that the observed optical activity in this case is due to an enhancement effect in one of the diastereomers (the one that preferably forms, judging from the shape of the spectrum). A similar enhancement has been observed by Gellman et al. when studying the interaction of D- and L-cysteine-protected plasmonic Au nanoparticles and enantiopure propylene oxide.[19] Induction of optical activity on otherwise inactive metal clusters

dx.doi.org/10.1021/ja500809p | *J. Am. Chem. Soc.* 2014, 136, 4129−4132

has also been demonstrated in boronic acid-protected clusters via addition of fructose.[20] Apparently, strong interaction between ligands and chiral additives can effectively break the symmetry of the system and induces optical activity. When using rather inert ligands such as phenylethanethiolate, no optical activity is observed even when dissolving the cluster in chiral solvents.[21]

The CD spectrum of a (left-handed) *A*-$Au_{102}(SR)_{44}$ cluster (with R = H as model ligand) was computed to compare to the experimental spectra obtained after partial phase transfer. All computations were performed using the projector-augmented wave method as implemented in the real space grid package GPAW.[22] Computations were performed at the DFT level. For this, the coordinates of the X-ray structure[1] were used, and the *p*-MBA ligands were replaced with SH. The structure was optimized by using the local density approximation (LDA), and the CD spectrum was calculated using a recently implemented[6,23−25] formulation of time-dependent DFT. A good agreement between simulation and experiment is found (Figure 3). The spectrum of the organic phase has the same sign as the

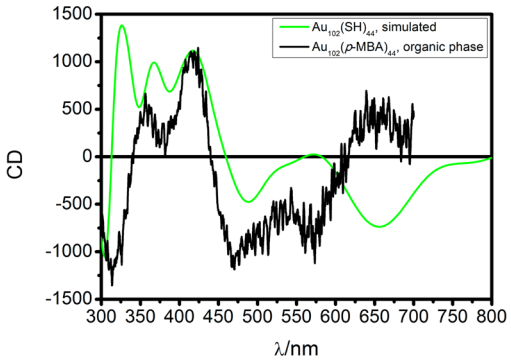

Figure 3. Comparison of the experimental CD spectrum (organic phase, black) after partial phase transfer and a computed spectrum of a left-handed model cluster, *A*-$Au_{102}(SH)_{44}$ (green). Overall, a good agreement is found, and assignment of handedness is possible. The full computed spectrum is shown in Figure S3.

Table 1. Comparison of Energy (in nm) and Sign in the CD Spectra of Party Phase-Transferred $Au_{102}(p\text{-MBA})_{44}$ Clusters (organic phase) and Computed *A*-$Au_{102}(SH)_{44}$

$Au_{102}(p\text{-MBA})_{44}$	*A*-$Au_{102}(SH)_{44}$
315 (−)	300 (−)
355 (+)	325 (+)
400 (+), shoulder only	365 (+)
415 (+)	415 (+)
470 (−)	490 (−)
570 (−)	655 (−)

computed one for most of the transitions (Table 1), and we therefore tentatively assign the enantiomer which is preferably transferred as the left-handed one (which was computed). Although the correspondence between the computed and measured CD spectra is not perfect, the computations allow for the assignment of the handedness. Slight deviations between the simulated and experimental spectra may be due to the use of a model ligand (SH instead of *p*-MBA), exclusion of solvent effects, or the presence of the chiral counterion in the experiment that is missing in the computations. Nevertheless, the overall agreement is good, and the predictive power of the applied DFT method is comparable to other computed CD spectra of smaller clusters.[6,24,26,27]

The presented results are of importance for application of thiolate-protected gold clusters in bioimaging. Monolayer-protected gold clusters and nanoparticles are widely deployed in molecular[13,28−30] and cellular electron microscopy.[31] They are investigated in preclinical imaging[14,32,33] and drug delivery or disease targeting applications.[12,34,35] In all of these investigations, the interaction of cluster chirality with the chiral nature of biomolecules is not yet examined. Thus it is completely unknown whether the handedness of a cluster affects its interaction with chiral molecules such as polynucleotides or proteins. It is likewise unknown if chirality affects targeting, circulation times, or clearance mechanisms. The facile approach for enantioenrichment of larger clusters presented here strongly suggests that these questions about how cluster chirality interacts with biological chirality are now within reach.

In summary, we present a facile method to enrich the enantiomers of intrinsically chiral, thiolate-protected gold clusters. Our target compound, $Au_{102}(p\text{-MBA})_{44}$ bears carboxyl groups in the ligand shell, which can interact with chiral ammonium ions ((−)-DME^+). A diastereoselective interaction forms hydrophobic ion pairs which can be transferred to chloroform. At suitable (low) concentration of (−)-DMEBr, only parts of the racemic cluster are transferred to the organic phase. Both the aqueous and organic phases show optical activity (of near mirror image relationship). At high concentrations of (−)-DMEBr, a full phase transfer is observed. The organic phase displays optical activity, which resembles the one of the organic phase after partial phase transfer. We assume the observation of optical activity after full phase transfer to be an enhancement effect in one of the diastereomers (most likely the more stable one). Computations give further confidence into the experimental spectra and allow a (tentative) assignment of handedness. We assign the enantiomer which is preferably phase transferred as the left-handed one, *A*-$Au_{102}(p\text{-MBA})_{44}$. Future studies will quantify the phase transfer and observation of optical activity (e.g., by screening the concentration of (−)-DMEBr).

■ ASSOCIATED CONTENT

Supporting Information

Experimental and computational details, additional spectra and full ref 22. This material is available free of charge via the Internet at http://pubs.acs.org

■ AUTHOR INFORMATION

Corresponding Authors

stefan.knoppe@chem.kuleuven.be
ackerson@mail.colostate.edu

Notes

The authors declare no competing financial interest.

■ ACKNOWLEDGMENTS

We gratefully acknowledge financial support from KU Leuven, Colorado State University, the University of Geneva and the University of Jyväskylä, and the Academy of Finland. S.K. is grateful to the DAAD for a postdoctoral fellowship. S.M. and H.H. thank L. Lehtovaara for discussions and technical help in the computations of the CD spectra. The computations were done at the HLRS computing center in Stuttgart as a part of a

PRACE project "Nano-gold at the bio-interface". Support from the Swiss National Foundation is acknowledged (T.B.).

REFERENCES

(1) Jadzinsky, P. D.; Calero, G.; Ackerson, C. J.; Bushnell, D. A.; Kornberg, R. D. *Science* **2007**, *318*, 430.
(2) Häkkinen, H.; Walter, M.; Grönbeck, H. *J. Phys. Chem. B* **2006**, *110*, 9927.
(3) Qian, H.; Eckenhoff, W. T.; Zhu, Y.; Pintauer, T.; Jin, R. *J. Am. Chem. Soc.* **2010**, *132*, 8280.
(4) Zeng, C.; Li, T.; Das, A.; Rosi, N. L.; Jin, R. *J. Am. Chem. Soc.* **2013**, *135*, 10011.
(5) Knoppe, S.; Dolamic, I.; Dass, A.; Bürgi, T. *Angew. Chem., Int. Ed.* **2012**, *51*, 7589.
(6) Malola, S.; Lehtovaara, L.; Knoppe, S.; Hu, K. J.; Palmer, R. E.; Bürgi, T.; Häkkinen, H. *J. Am. Chem. Soc.* **2012**, *134*, 19560.
(7) Dolamic, I.; Knoppe, S.; Dass, A.; Bürgi, T. *Nat. Commun.* **2012**, *3*, 798.
(8) Tsukuda, T. *Bull. Chem. Soc. Jpn.* **2012**, *85*, 151.
(9) Hulkko, E.; L.-A., O.; Koivisto, J.; Levi-Kalisman, Y.; Kornberg, R. D.; Pettersson, M.; Häkkinen, H. *J. Am. Chem. Soc.* **2011**, *133*, 3752.
(10) Zhu, M.; Aikens, C. M.; Hollander, F. J.; Schatz, G. C.; Jin, R. *J. Am. Chem. Soc.* **2008**, *130*, 5883.
(11) Knoppe, S.; Boudon, J.; Dolamic, I.; Dass, A.; Bürgi, T. *Anal. Chem.* **2011**, *83*, 5056.
(12) Simpson, C. A.; Salleng, K. J.; Cliffel, D. E.; Feldheim, D. L. *Nanomedicine* **2013**, *9*, 257.
(13) Hainfeld, J. F.; Furuya, F. R. *J. Histochem. Cytochem.* **1992**, *40*, 177.
(14) Hainfeld, J. F.; Slatkin, D. N.; Focella, T. M.; Smilowitz, H. M. *Brit. J. Radiol.* **2006**, *79*, 248.
(15) Heinecke, C. L.; Ni, T. W.; Malola, S.; Mäkinen, V.; Wong, O. A.; Häkkinen, H.; Ackerson, C. J. *J. Am. Chem. Soc.* **2012**, *134*, 13316.
(16) Yao, H.; Fukui, T.; Kimura, K. *J. Phys. Chem. C* **2008**, *112*, 16281.
(17) Brands, K. M.; Davies, A. J. *Chem. Rev.* **2006**, *106*, 2711.
(18) Varnholt, B.; Dolamic, I.; Knoppe, S.; Bürgi, T. *Nanoscale* **2013**, *5*, 9568.
(19) Shukla, N.; Bartel, M. A.; Gellman, A. J. *J. Am. Chem. Soc.* **2010**, *132*, 8575.
(20) Yao, H.; Saeki, M.; Kimura, K. *J. Phys. Chem. C* **2010**, *114*, 15909.
(21) Cao, T.; Jin, S.; Wang, S.; Zhang, D.; Meng, X.; Zhu, M. *Nanoscale* **2013**, *5*, 758.
(22) Enkovaara, J.; Rostgaard, C.; Mortensen, J. J.; et al. *J. Phys.: Condens. Matter* **2010**, *22*, 253202.
(23) Yang, H.; Wang, Y.; Huang, H.; Gell, L.; Lehtovaara, L.; Malola, S.; Häkkinen, H.; Zheng, N. *Nat. Commun.* **2013**, *4*, 2422.
(24) Knoppe, S.; Malola, S.; Lehtovaara, L.; Bürgi, T.; Häkkinen, H. *J. Phys. Chem. A* **2013**, *117*, 10526.
(25) Malola, S.; Lehtovaara, L.; Enkovaara, J.; Häkkinen, H. *ACS Nano* **2013**, *7*, 10263.
(26) Lopez-Acevedo, O.; Tsunoyama, H.; Tsukuda, T.; Häkkinen, H.; Aikens, C. M. *J. Am. Chem. Soc.* **2010**, *132*, 8210.
(27) Molina, B.; Sanchez-Castillo, A.; Knoppe, S.; Garzon, I. L.; Bürgi, T.; Tlahuice-Flores, A. *Nanoscale* **2013**, *5*, 10956.
(28) Ackerson, C. J.; Jadzinsky, P. D.; Jensen, G. J.; Kornberg, R. D. *J. Am. Chem. Soc.* **2006**, *128*, 2635.
(29) Ackerson, C. J.; Powell, R. D.; Hainfeld, J. F. *Meth. Enzymol.* **2010**, *481*, 195.
(30) Marjomäki, V.; Lahtinen, T.; Martikainen, M.; Koivisto, J.; Malola, S.; Salorinne, K.; Pettersson, M.; Häkkinen, H. *Proc. Natl. Acad. Sci. U.S.A.* **2014**, *111*, 1277.
(31) Nickell, S.; Kofler, C.; Leis, A. P.; Baumeister, W. *Nat. Rev. Mol. Cell Biol.* **2006**, *7*, 225.
(32) Hainfeld, J. F.; O'Connor, M. J.; Dilmanian, F. A.; Slatkin, D. N.; Adams, D. J.; Smilowitz, H. M. *Brit. J. Radiol.* **2011**, *84*, 526.
(33) Cullum, B. M.; Daniel, M.-C.; Aras, O.; Smith, M. F.; Nan, A.; Fleiter, T.; Porterfield, D. M.; Booksh, K. S. *Proc. SPIE* **2010**, *7674*, 76740J.
(34) Wong, O. A.; Hansen, R. J.; Ni, T. W.; Heinecke, C. L.; Compel, W. S.; Gustafson, D. L.; Ackerson, C. J. *Nanoscale* **2013**, *5*, 10525.
(35) Simpson, C. A.; Agrawal, A. C.; Balinski, A.; Harkness, K. M.; Cliffel, D. E. *ACS Nano* **2011**, *5*, 3577.